

NAFEES AHMED<sup>1</sup>  
MD. YASIN HOSSAIN<sup>1</sup>  
JOYANTA KUMAR SAHA<sup>1</sup>  
MOHAMMAD AL MAMUN<sup>1,2</sup>  
A. K. M. LUTFOR RAHMAN<sup>1</sup>  
JAMAL UDDIN<sup>3</sup>  
ABDUL AWAL<sup>1</sup>  
MD. SHAJAHAN<sup>1</sup>

<sup>1</sup>Department of Chemistry,  
Jagannath University, Dhaka,  
Bangladesh

<sup>2</sup>Nanotechnology and Catalysis  
Research Centre, Institute of  
Advanced Studies, University of  
Malaya, Kuala Lumpur, Malaysia

<sup>3</sup>Center for Nanotechnology,  
Chemistry, and Nanotechnology,  
Department of Natural Sciences,  
Coppin State University, Science  
and Technology Center,  
Baltimore, USA

SCIENTIFIC PAPER

UDC 677:544.4:66

## ADSORPTIVE REMOVAL OF CRYSTAL VIOLET DYE FROM AQUEOUS SOLUTION ONTO COCONUT COIR

### Article Highlights

- The dependence of pH on the adsorption mechanism of crystal violet on coconut coir was revealed
- The superiority of coconut coir in removing crystal violet from an aqueous solution was illuminated
- UT-CC and SCT-CC showed comparable removal capacity against crystal violet (CV) at high pH (8.00)
- The proposed adsorption mechanism of CV onto coconut coir was interpreted by FTIR data
- The DFT simulation revealed the interaction between CV and lignin in CC as chemisorption

### Abstract

*The untreated and sodium chlorite-treated coconut coir was implemented to remove crystal violet (CV) dye from an aqueous solution by batch adsorption experiments. The adsorption capacity, equilibrium time, and adsorption kinetics of CV on both adsorbents were regulated by the pH of the dye solution. High pH favors the comparative adsorption capacity for both adsorbents. In contrast, the untreated coconut coir (UT-CC) shows higher adsorption efficiency (9.61 mg g<sup>-1</sup>) than sodium chlorite-treated coconut coir (SCT-CC) at low pH. At lower pH (2.00), the equilibrium was established within 60 min by both adsorbents. However, the quick attainment of the equilibrium (30 min) was observed using both the adsorbents at higher pH (8.00). The isotherm data for both the adsorbents was found to have better agreement with the Freundlich than the Langmuir model at pH 8.00. The kinetic data was well-fitted with Ho's pseudo-second-order model. Both adsorbents were characterized by FTIR and SEM to get evidence for the proposed adsorption mechanism. Density functional theory (DFT) also supports this result which illustrates the adsorption of CV on lignin of CC with the adsorption energy -51.16 kJ/mol at the B3LYP/6-31(d,p) level of theory.*

*Keywords: coconut coir, sodium chlorite, crystal violet, adsorption kinetics, adsorption mechanism, density functional theory.*

The aquatic ecosystem is disturbed due to the interference in the penetration of light into the water and the degradation of the aesthetic value of water bodies caused by the color effluents discharged from dyeing

industries [1]. Carcinogenic and mutagenic dyes and pigments [2,3] are toxic that affect aquatic biota and humans [4]. It is difficult to degrade the dyes under natural conditions; therefore, the conventional wastewater treatment systems are not effective in typically removing these dyes. Dye effluents are currently treated by several physical or chemical techniques, such as microbial degradation, flocculation [5,6], membrane separation [7], ultra-chemical filtration [8], chemical oxidation, bioaccumulation, electrochemical treatment, adsorption, and reverse osmosis [9]. The wide range of dye-containing wastewater cannot be treated using most of these

Correspondence: Md. Shajahan, Department of Chemistry, Jagannath University, 9-10, Chittaranjan Avenue, Dhaka-1100, Bangladesh.

E-mail: [jahanms@chem.jnu.ac.bd](mailto:jahanms@chem.jnu.ac.bd); [jahanms@yahoo.com](mailto:jahanms@yahoo.com)

Paper received: 3 December, 2021

Paper revised: 26 April, 2022

Paper accepted: 6 June, 2022

<https://doi.org/10.2298/CICEQ211203009A>

techniques because of being costly and time-consuming. Moreover, dye biodegradation may produce by-products and/or other metabolites with higher toxicity than the primary substrate [10]. Other conventional techniques, such as coagulation and flocculation, do not help remove dyes from the water-introduced metallic impurities producing a large amount of sludge that requires further disposal.

Adsorption is one of the promising techniques for removing hazardous and environmentally undesirable chemicals [11]. Adsorption is generally chosen owing to easy handling, high efficiency, low energy input, and availability of different adsorbents [12,13]. Activated carbon from various sources (e.g., *Ricinus communis pericarp* [14]) is the most widely used adsorbent in removing the dye staff. However, it is not economically feasible. Therefore, low-cost and easily available bioadsorbents are usually used to remove dye staff in place of activated carbon at different operating conditions.

CV, a cationic textile dye, is an enhancer of bloody red fingerprints. It is applied to manufacture paints and printing inks [15]. Crystal violet is also used for preventing fungal growth in poultry feed [16,17]. In addition, skin infections by *Staphylococcus aureus* can be treated by CV [18,19]. However, crystal violet is carcinogenic like other textile dyes. Furthermore, it is classified as an intractable molecule since it is poorly metabolized by microbes, non-biodegradable, and can persist in various environments. Scientists have already investigated the removal of CV from the

wastewater by using different adsorbents, such as sugarcane bagasse [20], some waste materials, i.e., bottom ash [21], powdered mycelial biomass of *Ceriporia lacerata* P2 (CLB) [22]. So far, to the authors' knowledge, coconut coir, an environment-friendly bioadsorbent, has not been used to remove CV from the wastewater.

Therefore, low-cost and easily available coconut coir was used to remove CV from an aqueous solution. Coconut coir (as in dust, coir, or pith form) has been previously used to remove different dyes, such as malachite green [23], methylene blue, and remazol yellow [24]. But coconut coir, either raw or treated, has not been used to remove CV from the wastewater. Therefore, the present study not only portrayed the removal of CV from an aqueous solution using untreated coconut coir (UT-CC) and sodium chlorite-treated coconut coir (SCT-CC) but also shed light on the adsorption mechanism.

## MATERIAL AND METHODS

All chemicals were reagent grade. CV was obtained from Scharlau Chemicals, Spain. All the experimentation solutions were prepared by diluting stock solution. The preparation and dilution of CV solution were done with Distilled Deionized Water (DDW). The chemical specifications for CV are mentioned in Table 1.

The adsorbents employed in this research were

Table 1. . Chemical Specification for CV\*

## Crysta

Crystal violet, C.I. 42555		
VI0025	Crystal violet, C.I. 42555, indicator, extra pure	
	Synonyms: Hexamethylenepararosaniline chloride, Hexamethyl-p-rosanilinium chloride, Methyl violet 10 B $C_{25}H_{30}ClN_3$ $M = 407,99 \text{ g/mol}$ CAS [548-62-9] EINECS-No.: 208-953-6 Solub. in water: (20 °C): 10 g/l Melting point: 189 - 194 °C LD 50 (oral, rat): 420 mg/kg ADR: 9 M7 III UN 3077 IMDG: 9 III UN 3077 IATA/ICAO: 9 III UN 3077 GHS-signal word: Danger GHS-H sentences: H318 - H351 - H410 - H302 GHS-P sentences: P280 - P281 - P305 + P351 + P338 - P310 - P405 - P501a Tariff number: 3204 13 00 90	Applications: analytical chemistry, microscopy, indicator.  <b>Specifications:</b> dye content (spectrophotometric) ..... min. 85 % Absorption maximum $\lambda$ max (in $H_2O$ ) ... 589 - 594 nm Absorptivity (A 1%/1 cm; $\lambda$ max; 0,002 g/l; $H_2O$ ) ..... 2000 - 2450 loss on drying ..... max. 10 % suitability as indicator in TLC test ..... passes test non-aqueous solvents ..... passes test
<b>Art. No.</b>	<b>Volume</b>	<b>Container</b>
VI00250025	25 g	
VI00250100	100 g	

\*Chemicals and Reagents Index (page 150): Scharlau Chemicals, Spain (scharlab@scharlab.com)

UT-CC, i.e., raw coconut coir, and SCT-CC. The former was collected from the local market, whereas the latter

was obtained by treating the raw coir with sodium chlorite (80%  $NaClO_2$ , BDH laboratory, England).

Furthermore, instruments including a pH meter (Yangzhong SHI YIBIAO QIJIAN CHANG), a combination electrode with a precession of  $\pm 0.01$  pH units, and a UV-visible Spectrometer (OPTIZEN, Korea), were employed for measurement of pH and concentration of dye solution, respectively. In addition, scanning electron microscopic (SEM) analysis of the adsorbents was done with the help of an SEM -JEOL JSM 7600F electron microscope (JEOL, USA), while the recording of the IR spectrum of coconut coir was done with FT-IR Spectrometer [Model: Frontier FT-NIR/MIR] (Perkin Elmer, USA).

The raw fiber collected from the local market was washed with tap water followed by distilled water several times to remove dust and pigments. The washed fiber was sun-dried and then heated in an oven at  $110\text{ }^{\circ}\text{C}$ . The dried fiber was ground by a mechanical grinder and screened out to the desired mesh size using sieves of 150 and  $300\text{ }\mu\text{m}$  BSS mesh. The fiber, termed UT-CC, was kept in a desiccator until use.

The UT-CC was treated according to Box-Behnken's experimental design [25]. In this case, 6.2 g of  $\text{NaClO}_2$  was dissolved in distilled water in a three-neck flask, followed by adding 9.5 mL of acetic acid (99%) and stirring for about 60 min at  $90\text{ }^{\circ}\text{C}$  after adding 10 g of UT-CC. The treated coconut coir (SCT-CC) was washed thoroughly with distilled water until the filtrate reached pH at the neutral point, then dried the coir at  $70\text{ }^{\circ}\text{C}$  to a constant weight, screened through a sieve, and kept in desiccators for further use.

Preliminary investigations of the CV adsorption (equilibrium time and adsorption isotherm) onto UT-CC and SCT-CC helped select the optimum concentration and pH. The batch adsorption studies were carried out at three different pH values, 2.00, 7.00, and 8.00, by taking 40 mL of the dye solutions (100 mg/L) in a 250 mL reagent bottle and adding the adsorbents of selected mesh size ( $150\text{--}300\text{ }\mu\text{m}$  BSS) in the appropriate dosage (0.3 g) at room temperature ( $28.0\pm 0.5\text{ }^{\circ}\text{C}$ ). These dye solutions were shaken for a specific time at the desired speed. The adsorbent dose, contact time, and temperature during adsorption were carefully controlled. After centrifugation, the concentration of the dye solution was analyzed by a UV-Visible spectrophotometer (OPTIZEN, Korea). Absorptions were measured at the wavelengths of 590 nm for pH 7.00/8.00 and 625 nm for pH 2.00. These experiments were carried out with different dye concentrations ranging from 40–150 mg/L.

Kinetic measurements were made by taking 40 mL of the dye solutions in 250 mL reagent bottles and adding 0.3 g adsorbent (UT-CC or SCT-CC) for each run. The solutions were shaken at regular intervals, and after centrifugation, the supernatant

liquid was analyzed by a UV-visible spectrophotometer. Dye uptake was calculated from the concentration change of the dye solution before and after adsorption. For the kinetic studies, dye adsorption experiments were conducted at three different pH values, i.e., 2.00, 7.00, and 8.00.

FTIR spectra of the samples were recorded on a Frontier FT-NIR/MIR (Perkin Elmer, USA) spectrometer using potassium bromide pellets. The surface morphologies were determined using SEM (JSM 5600 LV, JEOL, USA) instrument with gold film.

## RESULTS AND DISCUSSION

### Adsorbent characterization

#### FTIR analysis of adsorbents

Coconut coir is composed of cellulose, hemicellulose, and lignin. FTIR analysis of the bare surface was carried out to know the surface functional groups. The investigated FTIR spectra of raw and treated fiber are shown in Figure 1. It was observed that the surface contained alcoholic (-OH) group [ $3449.7\text{ cm}^{-1}$ ], carbon-hydrogen bond {-C-H (stretch)} in alkane [ $2934.0\text{ cm}^{-1}$ ], carbon-hydrogen bond {-C-H (stretch)} in aldehyde group (-CHO) [ $2850.3\text{ cm}^{-1}$ ], carbon-carbon double bond (>C=C<) [ $1602.9\text{ cm}^{-1}$ ] and ethereal group (-O-) [ $1237.5\text{ cm}^{-1}$ ] [26]. According to the previous report, the oxidation of lignin was rendered by chlorine dioxide produced by  $\text{NaClO}_2$  after treating the fiber under acidic conditions [27]. The broadband at about  $3397\text{ cm}^{-1}$  attributed to the stretching vibration of -OH in cellulose became broader after treatment, possibly due to part of hydrogen bonds and lignin being broken [25]. This information indicated that the treatment broke lignin in the coconut coir.

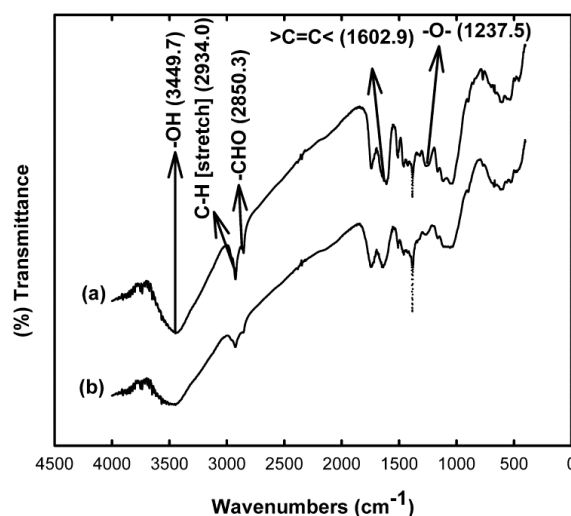


Figure 1. FTIR spectra of (a) UT-CC and (b) SCT-CC.

### SEM Analysis

SEM micrographs of UT-CC and SCT-CC are shown in Figure 2. The tube-like shape for UT-CC was observed in Figure 2(a). The shape of the coir remained unchanged after being treated with NaClO<sub>2</sub> (Figure 2(b)). However, some porous structures were observed after the treatment, indicating the treatment altered the surface morphology of coconut coir fiber. The result was dissimilar to the previously published article on

kapok fiber [25]. SEM photographs revealed the porosity and adsorptive nature of coconut coir. Due to the evolution of the porous site, the surface of SCT-CC became more conducive for the dye molecule to adsorb onto it rather than UT-CC. The porous morphology of SCT-CC observed in the SEM image was justified by the BET analysis shown in Table 2. EDS analysis shown the elementary composition of SCT-CC (Table 3).

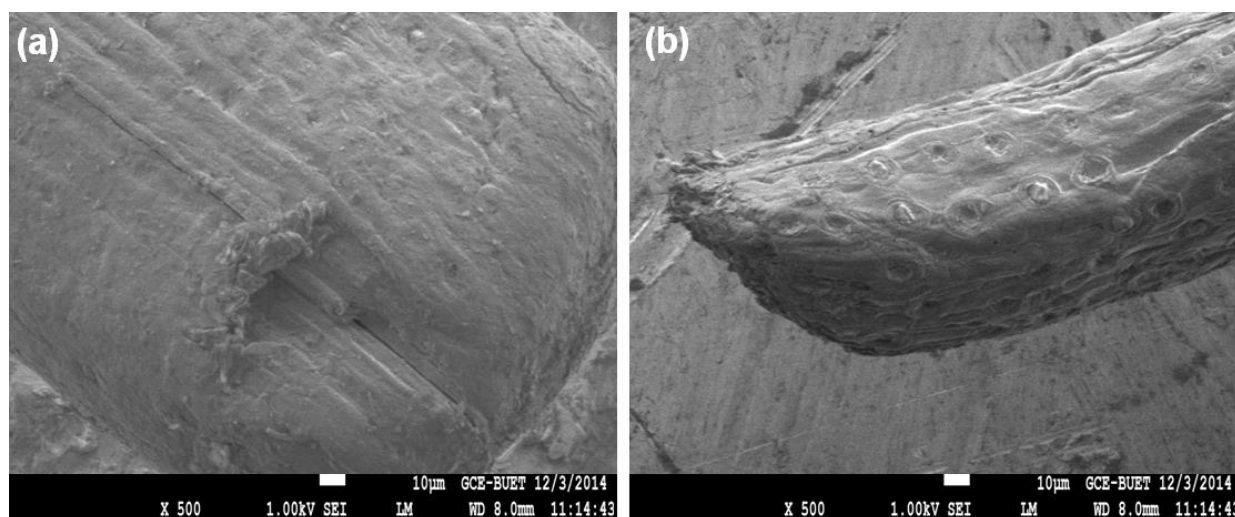


Figure 2. SEM micrographs of (a) UT-CC and (b) SCT-CC x 500 magnification.

Table 2. Summary of BET results of sodium chlorite treated coconut coir (SCT-CC)

Parameters	SCT-CC
BET-specific surface area (m <sup>2</sup> /g)	6.48
Total pore volume (cc/g)	0.0652
Skeletal density (g/cc)	2.2845
Porosity based on skeletal density (per gram of sample)	0.1297
Average pore diameter (Å)	402.2296

Table 3. The elementary composition of SCT-CC obtained from EDS analysis

ZAF Method Standardless Quantitative Analysis					
Fitting Coefficient : 0.0424					
Element	(keV)	Mass %	Sigma	Atom %	K
C K	0.277	52.17	0.19	59.86	51.5228
O K	0.525	45.35	0.36	39.06	44.0002
Na K	1.041	0.25	0.03	0.15	0.2975
Si K	1.739	0.54	0.03	0.27	0.8945
Cl K	2.621	1.69	0.05	0.66	3.2850
Total		100.0		100.0	

### Adsorption studies

#### Equilibrium time

The adsorption studies were carried out with UT-

CC and SCT-CC at different pH values. The adsorption process was rapid and reached equilibrium within 60 min for both the adsorbents at pH 2.00 (Figure 3(a)).

However, the attainment of the equilibrium adsorption was found to be somewhat faster (30 min) at high pH values for both the adsorbents (Figure 3(b)). Experiments at low pH using SCT-CC showed gradual adsorption of CV up to equilibrium, revealing that the surface's active site became porous after treatment. On the other hand, the discontinuous adsorption phenomenon was observed with UT-CC because of the absence of such an active porous site.

#### Factors affecting the amount adsorbed

The amount adsorbed of CV was affected by several factors, such as adsorbents, the pH of the adsorbate solution, and the initial concentration of the adsorbate solution. A significant difference in the removal capacity of CV for both adsorbents, e.g., UT-CC and SCT-CC, is depicted in Figure 3(a). It shows that UT-CC ( $9.61 \text{ mg g}^{-1}$ ) is a better adsorbent than SCT-CC ( $1.01 \text{ mg g}^{-1}$ ) for the adsorption of CV at pH 2.00. However, both the adsorbents were found to

have comparable adsorption capacity at pH 8.00 ( $12.45 \text{ mg g}^{-1}$  and  $13.54 \text{ mg g}^{-1}$  for UT-CC and SCT-CC, respectively).

The value of pH has a pronounced effect on surface phenomena. Adsorption of the dye was dependent on the pH of the adsorbate solution. The tests at different pH values (from 2.00 to 8.00) at an initial dye concentration of  $100 \text{ mg/L}$  determined the suitable pH for adsorption. In the present work, it was proved experimentally that the change in pH from lower to higher (2.00 to 8.00) caused the increase in the effective removal of CV by adsorption on both the adsorbents (UT-CC: 96.48%, and SCT-CC: 98.26%). It was found that the amount adsorbed ( $q_t$ ) was lower at lower pH than the higher pH for both UT-CC and SCT-CC depicted in Figure 3(a). But the adsorption capability and the rate of adsorption pronouncedly

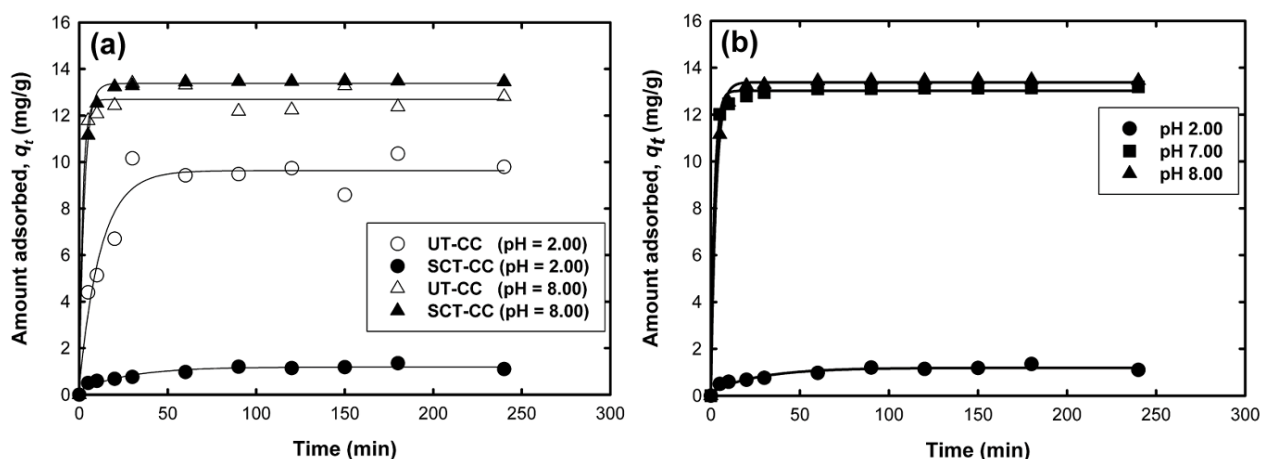


Figure 3. (a) Amount of CV adsorbed per gram of UT-CC and SCT-CC at pH 2.00 and 8.00 at room temperature ( $28 \pm 0.5 \text{ }^\circ\text{C}$ ); (b) Amount of CV adsorbed per gram of SCT-CC at different pH values at room temperature ( $28 \pm 0.5 \text{ }^\circ\text{C}$ ).

increased for SCT-CC at higher pH conditions. The variation of amount adsorbed ( $q_t$ ) and equilibrium adsorbed amount ( $q_e$ ) with pH for SCT-CC were shown in Figure 3(b) and Figure 4(a). Here both the amount adsorbed increases with increasing pH values. Since CV carries a positive charge on the nitrogen atom, the surface becomes positive at lower pH and generates a repulsive force between the adsorbate and the surface. But as the pH was increased to higher values, the surface became negatively charged, and CV felt the electrostatic force of attraction towards the surface. As a result, the amount adsorbed increased optimistically. It was reported that as pH increased, the dye solution's charge density decreased. Hence, the electrostatic repulsion between the positively charged dye molecule and the surface of the adsorbent lowered and increased dye sorption [28]. Similar results were also reported on

the adsorption of crystal violet by R. Ahmad (2009) [29].

Variation of the equilibrium amount of CV adsorbed per gram of SCT-CC at different pH values is depicted in Figure 4(a). The equilibrium adsorbed amount of CV increases with the pH from 2.00 to 8.00, and almost saturation arises at a pH higher than 7.00. A similar result was observed by using magnetic activated carbon [30]. However, similar findings were obtained for the adsorption of CV onto SDS-modified MNPs, where the adsorption efficiency decreased with an increase in the pH above  $\text{pH}_{\text{zpc}}$  [31]. The experimental results also indicate that the rate of adsorption of CV onto SCT-CC increases with increasing pH, which agrees with the result published by A. L. Prasad and T. Shanti, 2012 [32]. According to them, the adsorption capacity and rate constant tend to increase as the initial pH of the solution increases due

to the  $pH_{zpc}$  of the adsorbents, which has an acidic value favorable for cation adsorption [32].

The pronounced effect of the equilibrium amount adsorbed was obtained by varying initial dye concentration for both the adsorbents. Adsorption experiments for both adsorbents were carried out at room temperature ( $28 \pm 0.5$  °C) with an adsorbent dosage of 0.3 g in a concentration range of 40 to 150 mg/L. An increase in the concentration led to a rise in the amount of the adsorbed dye. This increase in adsorption with dye concentration is attributed to the retardation of resistance toward dye uptake, which increases the diffusion of the dye (Figure 4(b)). Figure 4(b) shows that the maximum adsorption of CV onto UT-CC is achieved at 150 ppm, whereas in the case of SCT-CC, the uptake increases further if the initial concentration of CV has been increased much. This finding can be compared with the results obtained from the removal of CV using a surfactant-modified magnetic nanoadsorbent [31], where the maximum removal of CV was 10 mg/L.

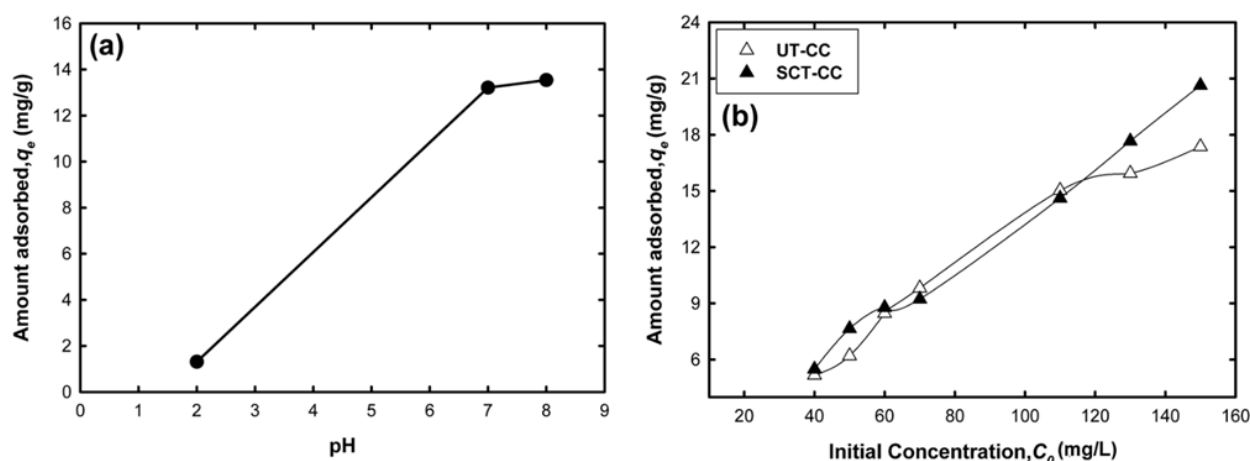


Figure 4. (a) Variation of the amount of CV dye adsorbed on SCT-CC as a function of pH; (b) Amount of CV dye adsorbed on UT-CC and SCT-CC with the varying initial concentration of dye at pH 8.00 at room temperature ( $28 \pm 0.5$  °C).

further adsorption occurs at that site [36]. It also suggests that all the adsorption sites are of equivalent energy, which the Langmuir Isotherm equation can explain –

$$\frac{x}{m} = \frac{aC_e}{1 + bC_e}$$

$$\frac{C_e}{x/m} = \frac{1}{kK_{eq}} + \frac{C_e}{k} \quad (1)$$

$$\text{or, } \frac{C_e}{q_e} = \frac{1}{q_m K_{eq}} + \frac{C_e}{q_m} \quad (2)$$

where,  $x/m$  - amount adsorbed;  $C_e$  - equilibrium concentration;  $k$  - rate constant;  $K_{eq}$  - equilibrium constant;  $q_e$  - amount adsorbed at equilibrium;  $q_m$  - amount adsorbed at monolayer;  $a$ ,  $b$  - Langmuir constants.

#### Freundlich isotherm

The Freundlich isotherm results from the

#### Adsorption isotherm

The most favored approach to an investigation of the adsorption mechanism is a study of the isotherm. The adsorption isotherm refers to the plot of the amount adsorbed against equilibrium concentration at a constant temperature [33]. The implication of the adsorption isotherms in the adsorption mechanism is based on a few aspects, such as the shape of the isotherm, the significance of the plateau in many isotherms, and the orientation of the adsorbed molecules [34,35]. The adsorption isotherms obtained for the adsorption of CV onto UT-CC and SCT-CC at pH 8.00 at room temperature ( $28 \pm 0.5$  °C) were justified based on the Langmuir and Freundlich isotherms model.

#### Langmuir isotherm

The Langmuir isotherm assumed that once the adsorbent site is covered with the dye molecules, no

assumption that the adsorption occurs on a heterogeneous surface, and non-uniform distribution of the heat of adsorption over the adsorbent surface takes place [37,38]. The Freundlich model was applied to calculate the adsorption data of CV, as per the given relation:

$$\frac{x}{m} = K_F C_e^{1/n} \quad (3)$$

$$\text{Or, } \log\left(\frac{x}{m}\right) = \log K_F + \frac{1}{n} \log C_e \quad (4)$$

The adsorption isotherm found experimentally was fitted relatively more precisely to Freundlich than to Langmuir isotherm for both experiments with UT-CC and SCT-CC at pH 8.00. In the case of UT-CC, the isotherm was found to be the Freundlich type rather

than the Langmuir model. On the other hand, the adsorption isotherm was found to match with both Langmuir and Freundlich isotherms (Figure 5, Table 4) in the case of SCT-CC. The Langmuir isotherm for UT-CC seemed to be quite similar to that of the removal of

CV using polyaniline nanoparticles at the temperature of 308 K with the value of  $R^2$  is 0.607 [39]. However, other research reported a higher value of  $R^2$  (0.99) at the temperature of 308 K for Langmuir isotherm [40].

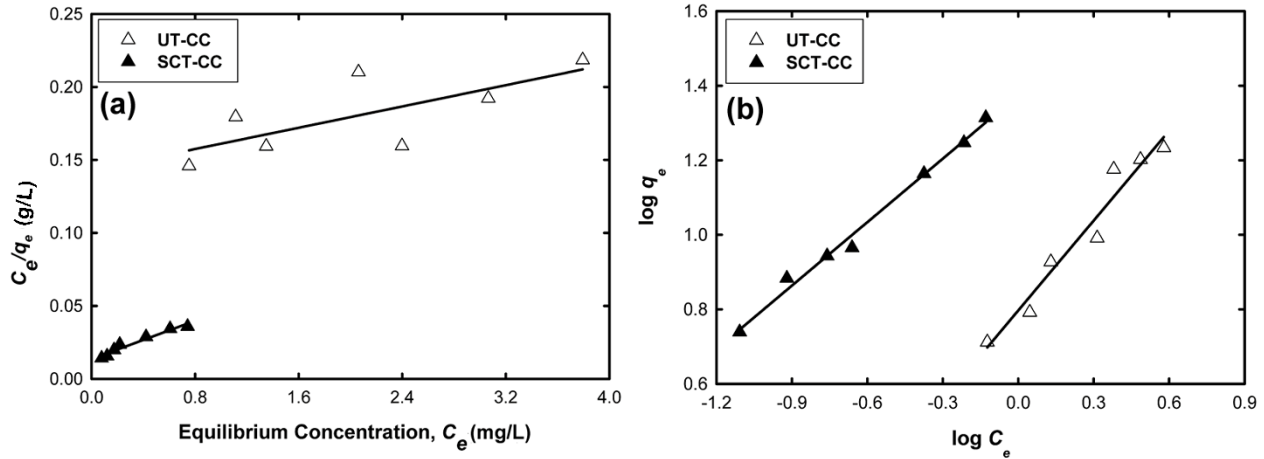


Figure 5. (a) A plot of  $\log C_e/q_e$  vs.  $C_e$  for fitting with Langmuir isotherm for the adsorption of CV on UT-CC and SCT-CC at pH 8.00; (b) A plot of  $\log q_e$  vs.  $\log C_e$  for fitting with Freundlich Isotherm for the adsorption of CV on UT-CC and SCT-CC at pH 8.00.

Table 4. Langmuir and Freundlich coefficients for the adsorption of crystal violet dye on untreated (UT-CC) and sodium chlorite treated (SCT-CC) coconut coir at pH 8.00 and room temperature ( $28 \pm 0.5$  °C)

Adsorbent	Langmuir Coefficients			Freundlich Coefficients		
	$q_m$ (mg/g)	$K_{eq}$ (L/mg)	$R^2$	$K_F$ (L/g)	$n$	$R^2$
UT-CC	54.94	0.13	0.528	6.26	1.24	0.952
SCT-CC	30.49	2.43	0.950	23.70	1.76	0.991

[N.B.:  $q_m$  - amount of CV adsorbed in monolayer;  $K_{eq}$  - equilibrium constant;  $R^2$  - correlation coefficient;  $K_F$  - Freundlich constant;  $n$  - adsorption intensity or number of layers formed.]

### Adsorption kinetics

The adsorption kinetics is crucial for understanding the adsorption mechanism and the adsorbate uptake rate. The data obtained from the estimation of equilibrium time for the adsorption of CV on SCT-CC at pH 2.00, 7.00, and pH 8.00 were fitted in both Lagergren's first-order and Ho's pseudo-second-order kinetic equations [41], respectively:

$$\ln(q_e - q_t) = \ln q_e - k_1 t \quad (5)$$

and

$$\frac{t}{q_t} = \frac{1}{k_2 q_e^2} + \frac{t}{q_e} \quad (6)$$

where  $q_e$  and  $q_t$  denote the amounts adsorbed at equilibrium and at any time  $t$ , respectively, and  $k_1$  and  $k_2$  are the first-order and second-order rate constants.

The data for first- and second-order kinetics at different pH were depicted in Figures 6(a) and 6(b), respectively. The values of the correlation coefficient,  $R^2$  (indicated in Table 5), revealed that the adsorption kinetics of CV onto SCT-CC mostly follow Ho's pseudo-

second-order kinetics model at all pH.

### Adsorption thermodynamics

Thermodynamics determines the different parameters, such as internal energy, enthalpy, entropy, and free energy values of the system, during physical or chemical transformation, which examines how they depend on the reaction conditions. The reaction's spontaneity can be understood by studying the thermal properties of the reactants, such as entropy and enthalpy, to obtain information about the equilibrium. Thermodynamic parameters, such as the change in free energy ( $\Delta G$ ), enthalpy ( $\Delta H$ ), and entropy ( $\Delta S$ ), are calculated by using the following equations:

$$K_d = \frac{q_e}{C_e} \quad (7)$$

$$\Delta G = -RT \ln K_d \quad (8)$$

$$\Delta G = \Delta H - T\Delta S \quad (9)$$

where  $R$  is the universal gas constant (8.314 J/mol K),  $T$  is the temperature (K),  $K_d$  is the distribution coefficient for the adsorption,  $\Delta G$  is the change in free energy

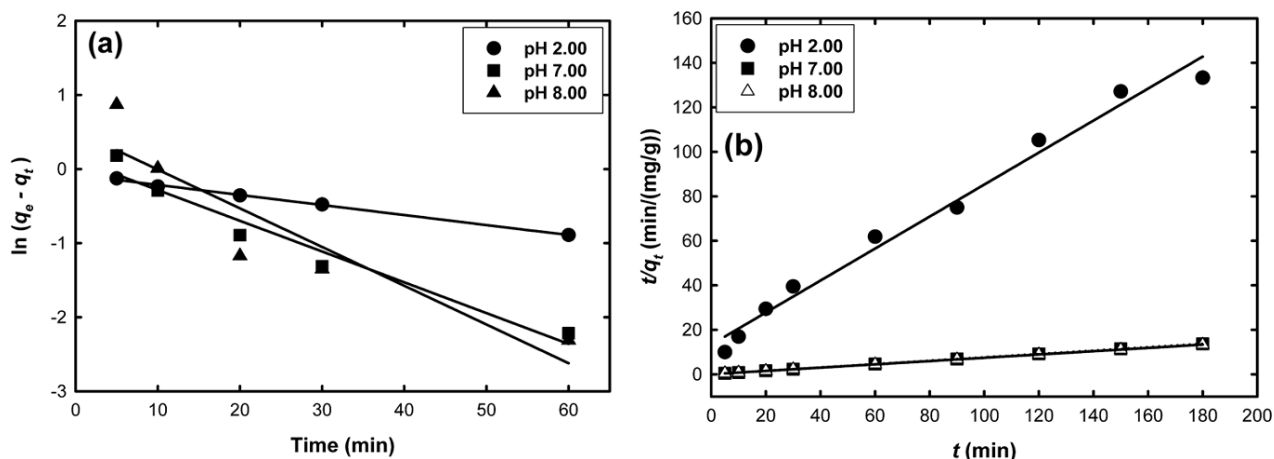


Figure 6. (a) A plot of  $\ln(q_e - q_t)$  vs. time for fitting with Lagergren equation of first-order kinetics for adsorption of CV on SCT-CC at pH 2.00, 7.00, and 8.00; (b) A plot of  $t/q_t$  vs. time for fitting with Ho's equation of pseudo-second-order kinetics for adsorption of CV on SCT-CC at pH 2.00, 7.00 and 8.00.

Table 5. Pseudo first order and pseudo-second order kinetic parameters for the adsorption of crystal violet dye onto SCT-CC at different pH values

pH	$q_e$ (mg/g)	Pseudo-first-order kinetic model		Pseudo-second-order kinetic model	
		$k_1$ ( $\text{min}^{-1}$ )	$R^2$	$k_2$ ( $\text{g l}/(\text{mg min})$ )	$R^2$
2.00	1.24	$1.80 \times 10^{-2}$	0.996	$3.87 \times 10^{-2}$	0.982
7.00	13.21	$4.15 \times 10^{-2}$	0.936	$14.65 \times 10^{-2}$	1.000
8.00	13.54	$5.23 \times 10^{-2}$	0.789	$10.62 \times 10^{-2}$	1.000

[N.B.:  $q_e$  - amount of CV adsorbed at equilibrium;  $k_1$  - first order rate constant;  $k_2$  - second order rate constant;  $R^2$  - correlation coefficient]

(kJ/mole),  $\Delta H$  is the change in enthalpy (kJ/mole), and  $\Delta S$  is the change in entropy (kJ/mol K).

The value of  $\Delta G$  can be determined by Eq. (9). As the authors did the thermodynamic study at room temperature only, they studied the variation of the value of  $\Delta G$  for different adsorbents at different pH values. A more negative value of  $\Delta G$  for SCT-CC at a high pH indicates how the basic medium is conducive to the spontaneity of the system. The data for free energy at different conditions are incorporated in Table 6.

Table 6. Data for the free energy of the Coir-CV system at room temperature ( $28 \pm 0.5$  °C) at different pH values

Adsorbents	Free energy, $\Delta G$ (kJ/mol)		
	pH		
	2.00	7.00	8.00
UT-CC	-1.833.1	-	-7.947.4
SCT-CC	5.677.49	-10.153	-12.794

### Adsorption mechanism

The FTIR studies have confirmed the existence of hydroxyl (-OH), aldehyde (-CHO), and ether (-O-) groups of lignin in UT-CC and SCT-CC. The biosorption

of CV onto UT-CC and SCT-CC may likely be due to the electrostatic force of attraction between these groups and the cationic dye molecules. The hydroxyl groups become more polar at a high pH (i.e., 7.00 and 8.00). Hence, partially charged hydroxyl can attract the positively charged dye molecules, and binding can occur through H-bond (Figure 7). At pH 2.00, the peak for ether (-O-) at  $1237.5 \text{ cm}^{-1}$  diminished after adsorption (Figure 7(a) ii), which revealed that in acidic conditions, the ethereal group is protonated, and thus the absorption peak disappeared. There is a weak electrostatic interaction between the dyes and the electron-rich sites of the adsorbent surface, i.e., ether (-O-) groups. The FTIR spectrum shows that the peak for carbon-hydrogen bond {-C-H (stretch)} in -CHO at  $2860.2 \text{ cm}^{-1}$  almost diminishes after adsorption at pH 8 (Figure 7(a) iii), which indicates the van der Waals interaction between polar -HCO group (i.e., aldehyde) and cationic dye, CV.

The FTIR data for the bare SCT-CC in Figure 7(b) illustrates that the broad band at about  $3449.7 \text{ cm}^{-1}$  (mentioned in Figure 1) became sharpened as the pH of the adsorbate solution was increased from 2.00 to 8.00 (Figure 7(b) ii-iv). It might be owing to the reformation of a hydrogen bond. On the other hand, the

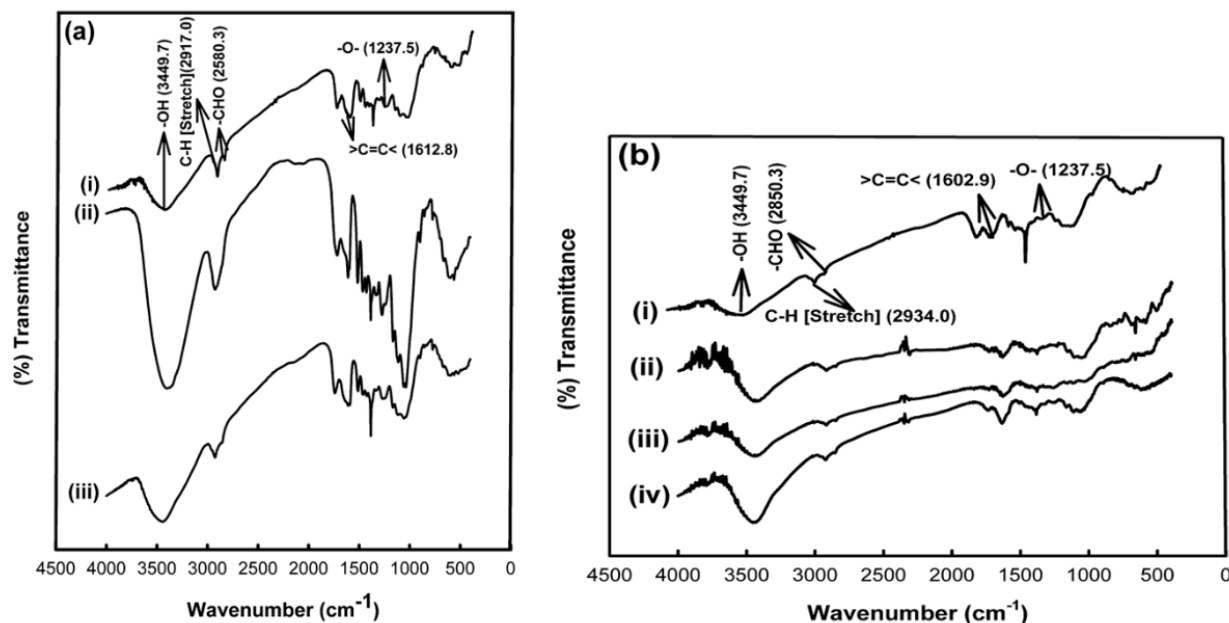


Figure 7. (a) FTIR Spectra of (i) bare UT-CC and CV-adsorbed UT-CC at (ii) pH 2.00 and (iii) pH 8.00; (b) FTIR Spectra of (i) bare SCT-CC and CV-adsorbed SCT-CC at (ii) pH 2.00 and (iii) pH 7.00 and (iv) pH 8.00.

band at  $1737\text{ cm}^{-1}$  in bare SCT-CC, which indicates the existence of aldehydic C=O (Figure 7(b) i) [26], completely diminishes at pH 2.00 because of the protonation of the surface at low pH. On the other hand, the surface becomes conducive to adsorbing cationic dye, CV at pH 8.00 (Figure 7(b) iii). As a result, the peak for aldehydic C=O has a lower intensity, and its frequency shifts to the lower wavenumber ( $1732.5\text{ cm}^{-1}$ ). It may be due to the electrostatic interaction between negatively charged SCT-CC and cationic dye, CV.

#### DFT simulation

The adsorption scenario of  $\text{CV}^+$  (cationic form) on UT-CC was performed using a density functional theory (DFT) study. A lignin molecule of CC was considered to interact with  $\text{CV}^+$ . Firstly, the lignin molecule of CC and a  $\text{CV}^+$  molecule were optimized separately using B3LYP [42,43] functional, and the basis set 6-31G(d,p). Then,  $\text{CV}^+$  was kept on top of the lignin molecule at a certain distance to interact. Figure 8(a) shows the optimized structure of the lignin- $\text{CV}^+$  complex where

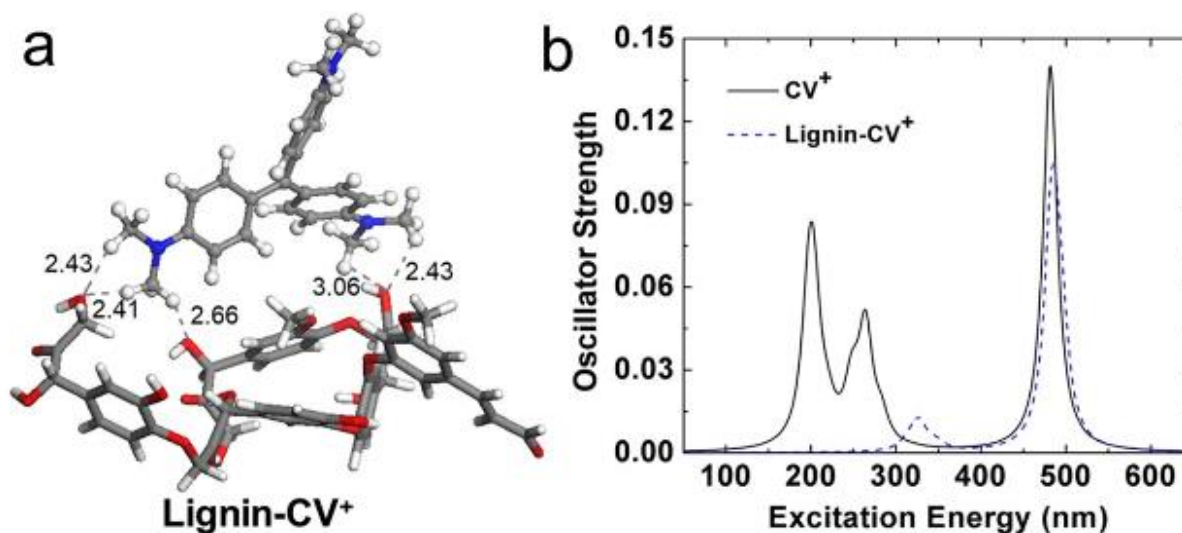


Figure 8. (a) Adsorption of  $\text{CV}^+$  (ball and stick model) on lignin (stick model); (b) UV-vis spectrum of lignin- $\text{CV}^+$  complex. In figure 8(b), the solid line represents the adsorption spectrum of pristine  $\text{CV}^+$  and the dotted line for the lignin- $\text{CV}^+$  complex.

CV<sup>+</sup> interacts with lignin through hydrogen bonds. The adsorption energy ( $\Delta E_{ad}$ ) was calculated by subtracting the total energy of lignin and CV<sup>+</sup> from that of the lignin-CV<sup>+</sup> complex. The calculated adsorption energy is -51.16 kJ/mol. Natural bond orbital (NBO) analysis reasserts that during adsorption of CV<sup>+</sup> on lignin, CV detracts 0.033e- charges from lignin. The amount of this charge transfer measures the strength of the interaction between lignin and CV<sup>+</sup> [44]. The adsorption spectra of pristine CV<sup>+</sup> and lignin-CV<sup>+</sup> complex were calculated using TD-DFT with the above-mentioned level of theory to confirm this interaction. The estimated  $\lambda_{max}$  for the pristine CV<sup>+</sup> was found at 482 nm with two low-intensity bands at 201 nm and 264 nm (Figure 8(b)). When CV<sup>+</sup> interacts with lignin,  $\lambda_{max}$  was red-shifted by only 2.0 nm, but the two low-intensity bands of pristine CV<sup>+</sup> diminished towards a weak band and red-shifted at 326 nm. This red shifting and newly appeared weak band for the lignin-CV<sup>+</sup> complex confirms the interaction between CV<sup>+</sup> and lignin. All DFT calculations were carried out using Gaussian16 [45].

## CONCLUSION

The adsorption of CV on UT-CC and SCT-CC at different pH values in the batch method was investigated by studying the analytical data and some experimental evidence. On the other hand, the authors also explain the superiority of UT-CC and SCT-CC in removing CV from an aqueous solution by setting a particular experimental condition. Though at lower pH (2.00), UT-CC was observed to be a better adsorbent than SCT-CC in removing CV from aqueous solution, both of these adsorbents showed comparable removal capacity of CV at higher pH (8.00) by the quick attainment (within 30 min) of the equilibrium. Furthermore, the treatment of coconut coir by sodium chlorite brought some change in coir, evidenced by the FTIR data and SEM images. According to the experimental data and other findings, the authors believe that SCT-CC can be treated as a relatively better adsorbent than UT-CC under basic conditions. Using DFT calculation, the calculated adsorption energy of CV on lignin of CC was found to be -51.16 kJ/mol, and the adsorption (of CV on lignin of CC) was confirmed by the calculated adsorption spectra, where the  $\lambda_{max}$  of pristine CV red-shifted after its adsorption.

## Acknowledgment

The authors are indebted to Jagannath University for funding for this research. In addition, the authors acknowledge the cooperation provided by the 20

Department of Chemistry, the University of Dhaka in analyzing the FTIR data of the samples, and the Department of Glass and Ceramic, Bangladesh University of Engineering and Technology for taking SEM images of the samples.

## REFERENCES

- [1] J.H. Weisburger, *Mutat. Res.* 506-507 (2002) 9–20. [https://doi.org/10.1016/S0027-5107\(02\)00147-1](https://doi.org/10.1016/S0027-5107(02)00147-1)
- [2] R.O. Alves de Lima, A. P. Bazo, D.M.F. Salvadori, C. M. Rech, O. Danielle de Palma, U. Gisela de Aragao, *Mut. Res.* 626 (2007) 53–60. <https://doi.org/10.1016/j.mrgentox.2006.08.002>
- [3] N. Mathur, P. Bhatnagar, P. Sharma, *Univ. J. Environ. Res. Technol.* 2(2) (2012) 1–18. <https://www.environmentaljournal.org/2-2/ujert-2-2-1.pdf>
- [4] B. Lellis, C.Z. Fávoro-Polonio, J.A. Pamphile, J.C. Polonio, *Biotechnol. Res. Innov.* 3(2) (2019) 275–290. <https://doi.org/10.1016/j.biori.2019.09.001>
- [5] M. Sudha, A. Saranya, G. Selvakumar, N. Sivakumar, *Int. J. Curr. Microbiol. App. Sci.* 3(2) (2014) 670–690. <https://www.ijcmas.com/vol-3-2/M.Sudha,%20et%20al.pdf>
- [6] S. P. Upadhyay, *J. Environ. Res. Dev.* 3(2) (2008) 490–494. <http://www.jerad.org/ppapers/V003N002/V003N002P0490.pdf>
- [7] A. Gurses, C. Dogar, M. Yalcin, M. Acikyildiz, R. Bayrak, S. Karaca, *J. Hazard. Mater.* 131(6) (2006) 217–228. <https://doi.org/10.1016/j.jhazmat.2005.09.036>
- [8] C. Allegre, P. Moulin, M. Maisseu, F. Charbit, *J. Membr. Sci.* 269(4) (2006) 15–34. <https://doi.org/10.1016/j.memsci.2005.06.014>
- [9] K. Kadirvelu, K. Thamaraiselvi, C. Namasivayam, *Bioresour. Technol.* 76 (2001) 63–65. [https://doi.org/10.1016/S0960-8524\(00\)00072-9](https://doi.org/10.1016/S0960-8524(00)00072-9)
- [10] J.A. Ramsay, T. Nguyen, *Biotech. Lett.* 24(21) (2002) 1757–1761. <https://doi.org/10.1023/A:1020644817514>
- [11] K.B. Hu, Y.L. Wang, C.R. Li, Y.Q. Zheng, *Acta Sci. Circumstantiae* 30(11) (2010) 2174–2183. [http://caod.oriprobe.com/articles/25753718/Fractal\\_characteristics\\_of\\_adsorption\\_of\\_direct\\_dye\\_compounds\\_onto\\_mod.htm](http://caod.oriprobe.com/articles/25753718/Fractal_characteristics_of_adsorption_of_direct_dye_compounds_onto_mod.htm)
- [12] E. Bascetin, G. Atun, *J. Chem. Eng. Data* 55 (2010) 783–788. <https://doi.org/10.1021/je9004678>
- [13] M.L. Zanota, N. Heymans, F. Gilles, B.L. Su, M. Frer, G.D. Weireld, *J. Chem. Eng. Data* 55 (2010) 448–458. <https://doi.org/10.1021/je900539m>
- [14] S. Madhavakrishnan, K. Manickavasagam, R. Vasanthakumar, K. Rasappan, R. Mohanraj, S. Pattabhi, *e-J. Chem.* 6(4) (2009) 1109–1116. <https://doi.org/10.1155/2009/764197>
- [15] A. Adak, M. Bandyopadhyay, A. Pal, *Sep. Purif. Technol.* 44(2) (2005) 139–144. <https://doi.org/10.1016/j.seppur.2005.01.002>
- [16] C.D. Lin, C.T. Chen, *Anim. Feed Sci. Technol.* 54 (1995) 217–226. [https://doi.org/10.1016/0377-8401\(94\)00760-7](https://doi.org/10.1016/0377-8401(94)00760-7)
- [17] C.L. Hall, P.B. Hamilton, *Poult. Sci.* 6 (1982) 62–66. <https://doi.org/10.3382/ps.0610062>
- [18] R.L. Berrios, J.L. Arbiser, *Dermatol. Clin.* 29(1) (2011) 69–73. <https://doi.org/10.1016/j.det.2010.08.009>
- [19] A. Pona, E.Y. Quan, A. Cline, S.R. Feldman, *Dermatol Online J.* 26(5) (2020) 13030.

- <https://doi.org/10.5070/D3265048772>
- [20] P. Das, S. Chakraborty, S. Chowdhury, Arch. Environ. Sci. 6 (2012) 57–61. <https://aes.asia.edu.tw/Issues/AES2012/SahaPD2012-1.pdf>
- [21] A. Mittal, J. Mittal, A. Malviya, D. Kaur, V.K. Gupta, J. Colloid Interface Sci. 343 (2009) 463–473. <https://doi.org/10.1016/j.jcis.2009.11.060>
- [22] Y. Lin, X. He, G. Han, Q. Tian, W. Hu, J. Environ. Sci. 23(12) (2011) 2055–2062. [https://doi.org/10.1016/S1001-0742\(10\)60643-2](https://doi.org/10.1016/S1001-0742(10)60643-2)
- [23] U.J. Etim, E. Inam, S.A. Umoren, U.M. Eduok, Int. J. Environ. Bioenergy 5(2) (2013) 62–79. <https://modernscientificpress.com/Journals/ViewArticle.aspx?gkN1Z6Pb60HNQPymfPQIZF418S3XB/1Y/g5SJrtEz9tnj9x30LtKANTNh7z40/x>
- [24] J. de Souza Macedo, C.J. Nivan B. da, E.A. Luis, S.V. Eunice F. da, R.C. Antonio, F.G. Iara de, V.C. Neftali L., S.B. Ledjane, J. Colloid Interface Sci. 298 (2006) 515–522. <https://doi.org/10.1016/j.jcis.2006.01.021>
- [25] L. Yi, W. Jintao, Z. Yian, W. Aiqin, Chem. Eng. J. 184 (2012) 248–255. <https://doi.org/10.1016/j.cej.2012.01.049>
- [26] D.L. Pavia, G.M. Lampman, G.S. Kriz, Introduction to Spectroscopy: A Guide for Students of Organic Chemistry, 3rd Ed, Thomson Learning, (2001), p. 26. <https://www.hdki.hr/download/repository/Pavia-Introduction-to-Spectroscopy%5B1%5D.pdf>
- [27] S. Keshk, W. Suwinarti, K. Sameshima, Carbohydr. Polym. 65 (2006) 202–206. <https://doi.org/10.1016/j.carbpol.2006.01.005>
- [28] A. Saeed, M. Sharif, M. Iqbal, J. Hazard. Mater. 179(1-3) (2010) 564–572. <https://doi.org/10.1016/j.jhazmat.2010.03.041>
- [29] R. Ahmad, J. Hazard. Mater. 171(1-3) (2009) 767–773. <https://doi.org/10.1016/j.jhazmat.2009.06.060>
- [30] S. Iman, S. Mahboube, S. Abolfazl, H. Mohsen, H. Saeed, Arab. J. Sci. Eng. 41 (2016) 2611–2621. <https://doi.org/10.1007/s13369-016-2109-3>
- [31] M. Chandrasekaran, M.S. Vaiyazhipalayam, T. Marimuthu, J. Taiwan Inst. Chem. Eng. 63 (2016) 354–362. <https://doi.org/10.1016/j.jtice.2016.03.034>
- [32] A.L. Prasad, T. Shanti, Sustain. Environ. Res. 22(2) (2012) 113–122.
- [33] S.H. Maron, C.F. Prutton, Principles of Physical Chemistry, MacMillan Publishing Co., (1972), p. 813.
- [34] R.A. Latour, J. Biomed. Mater. Res. A: 103A: (2015) 949–958. <https://doi.org/10.1002/jbm.a.35235>
- [35] M.B. Yahia, Y.B. Torkia, S. Knani, M.A. Hachicha, M. Khalfauoi, A.B. Lamine, Adsorpt. Sci. Technol. 31(4) (2013) 341–357. <https://doi.org/10.1260/0263-6174.31.4.341>
- [36] R.P.H. Gasser, An Introduction to Chemisorption and Catalysis by Metals, Oxford University Press, (1987), p. 12. ISBN 0198552718
- [37] N. Ayawei, S.S. Angaye, D. Wankasi, E.D. Dikio, Open J. Phys. Chem. 5(3) (2015a) 56–70. <https://doi.org/10.4236/ojpc.2015.53007>
- [38] N. Ayawei, A.T. Ekubo, D. Wankasi, E.D. Dikio, Orient. J. Chem. 31(30) (2015b) 1307–1318. <http://dx.doi.org/10.13005/ojpc/310307>
- [39] S. Muhammad, T. Hajira, K. Jawariya, H. Uzma, S. Atika, Ultrason. Sonochem. 34 (2017) 600–608. <https://doi.org/10.1016/j.ultsonch.2016.06.022>
- [40] S.R. Shirsath, A.P. Patil, B.A. Bhanvase, S.H. Sonawane, J. Environ. Chem. Eng. 3(2) (2015) 1152–1162. <https://doi.org/10.1016/j.jece.2015.04.016>
- [41] Y. Ho, G. McKay, Process Biochem. 34(5) (1999) 451–465. [https://doi.org/10.1016/S0032-9592\(98\)00112-5](https://doi.org/10.1016/S0032-9592(98)00112-5)
- [42] A.D. Becke, J. Chem. Phys. 98(7) (1993) 5648–5652. <https://doi.org/10.1063/1.464913>
- [43] C. Lee, W. Yang, R.G. Parr, Phys. Rev. B 37(2) (1988) 785–789. <https://doi.org/10.1103/physrevb.37.785>
- [44] J.K. Saha, M.S. Hossain, M.K. Ghosh, Struct. Chem. 30 (2019) 1427–1436. <https://doi.org/10.1007/s11224-018-1272-4>
- [45] M.J. Frisch, G.W. Trucks, H.B. Schlegel, G.E. Scuseria, M.A. Robb, J.R. Cheeseman, G. Scalmani, V. Barone, et al., Gaussian 16 Rev. C.01, Wallingford, CT (2016).

NAFEES AHMED<sup>1</sup>  
MD. YASIN HOSSAIN<sup>1</sup>  
JOYANTA KUMAR SAHA<sup>1</sup>  
MOHAMMAD AL MAMUN<sup>1,2</sup>  
A. K. M. LUTFOR RAHMAN<sup>1</sup>  
JAMAL UDDIN<sup>3</sup>  
ABDUL AWAL<sup>1</sup>  
MD. SHAJAHAN<sup>1</sup>

<sup>1</sup>Department of Chemistry,  
Jagannath University, Dhaka,  
Bangladesh

<sup>2</sup>Nanotechnology and Catalysis  
Research Centre, Institute of  
Advanced Studies, University of  
Malaya, Kuala Lumpur, Malaysia

<sup>3</sup>Center for Nanotechnology,  
Chemistry, and Nanotechnology,  
Department of Natural Sciences,  
Coppin State University, Science  
and Technology Center,  
Baltimore, USA

## UKLANJANJE BOJE KRISTAL VIOLET IZ VODENOG RASTVORA NA ADSORPCIJOM NA KOKOSOVOM VLAKNU

*Netretirana i kokosova vlakna obrađena natrijum-hloritom su primenjena za uklanjanje kristal violeta (CV) iz vodenog rastvora šaržnom adsorpcijom. Kapacitet adsorpcije, vreme ravnoteže i kinetika adsorpcije CV na oba adsorbenta su istraženi na kontrolisanim pH vrednostima rastvora boje. Visok pH poboljšava kapacitet adsorpcije oba adsorbenta. Nasuprot tome, pri niskoj pH vrednosti, neobrađena kokosova vlakna (UT-CC) pokazuju veću efikasnost adsorpcije ( $9,61 \text{ mg g}^{-1}$ ) nego kokosova vlakna obrađena natrijum-hloritom (SCT-CC). Na  $\text{pH} = 2,00$ , ravnoteža se uspostavlja za 60 min sa oba adsorbenta. Međutim, brže postizanje ravnoteže (30 min) primećeno je za adsorbenta na višem pH (8,00). Utvrđeno je da se podaci istraživanja ravnoteže pri pH 8,00 za oba adsorbenta bolje slažu sa Frojndlihovim nego sa Langmirovim modelom. Kinetički podaci se dobro slažu sa Huovim modelom pseudo-drugog reda. Oba adsorbenta su okarakterisana FTIR i SEM da bi se dobili dokazi za predloženi mehanizam adsorpcije. Teorija funkcionalne gustine (DFT), takođe, podržava ovaj rezultat koji ilustruje adsorpciju CV na ligninu kokosovog vlakna sa adsorpcionom energijom  $-51,16 \text{ kJ/mol}$  na nivou teorije B3LIP/6-31(d,p).*

*Ključne reči: kokosovo vlakno, natrijum-hlorit, kristal violet, kinetika adsorpcije, mehanizam adsorpcije, teorija funkcionalne gustine.*

NAUČNI RAD